STRAIN MEASUREMENTS OF CHONDRULES AND REFRACTORY INCLUSIONS IN ALLENDE.

Alastair W. Tait[1], Kent. R. Fisher[2], Justin I. Simon[3]. [1]Monash University, Clayton, Vic., 3800, Australia (alastair.tait@monash.edu), [2]University of Cincinnati, Cincinnati, OH, 45219 (kenton.r.fisher@NASA.gov), [3]Center for Isotope Cosmochemistry and Geochronology, ARES, NASA Johnson Space Center, Houston, TX 77058 TX 77058 (Justin.I.Simon@NASA.gov).

Introduction: This study uses traditional strain measurement techniques, combined with X-ray computerized tomography (CT), to evaluate petrographic evidence in the Allende *CV3* chondrite for preferred orientation and to measure strain in three dimensions. The existence of petrofabrics and lineations was first observed in carbonaceous meteorites in the 1960's [1]. Yet, fifty years later only a few studies have reported that meteorites record such features [2]. Impacts are often cited as the mechanism for this feature [3], although plastic deformation from overburden and nebular imbrication have also been proposed [1,4,5]. Previous work conducted on the Leoville *CV3* and the Parnallee *LL3* chondrites, exhibited a minimum uniaxial shortening of 33% and 21%, respectively [4,5]. Petrofabrics in Allende *CV3* have been looked at before; previous workers using Electron Back Scatter Diffraction (EBSD) found a major-axis alignment of olivine inside dark inclusions and an "augen"-like preferred orientation of olivine grains around more competent chondrules [6,7].

Methodology and Results: For this study a ~25 cm slab of the Allende *CV3* meteorite was chosen due to its unique size. Such a large sample size allows for observations on the near "outcrop" scale, allowing for observations to be made without the inherent sampling bias of thin-section studies.

Data Preparation. The slab was previously photographed at 13.88 μm/px resolution on both sides, with the CAIs digitized in Adobe Illustrator [8]. The slab was also subjected to X-ray tomography with a resolution of 173.91 μm/voxel. To reduce collection bias, components were identified by multiple workers and at different image orientations. There images were smaller statistically representations of the slab, as well as Scanning Electron Microscope (SEM) images. Components were grouped into Chondrules, Chondrule Rims and CAIs phase categories. Once the data was digitized, the images were processed in ImageJ [9], to record their physical characteristics: coordinates, area, major axis, minor axis, angle, circularity and solidity.

Finite Strain Analysis. Much of the strain analysis in this study borrows from methods laid out by Cain et al. (1986) that have been used in subsequent studies of meteorite fabric analysis [2,5]. Chondrules, CAIs and chondrule-rims had their Major/Minor axis ratios recorded. Harmonic means were used to reduce the effect of outliers in the sample populations (Table 1).

Table 1: Finite Strain Analysis Summary

Phase	Top (Tait) (Axial Ratio)	Top (Fisher) (Axial Ratio)	σ	± SE	Minimum Mean (Axial Ratio)	Uniaxial Shortening (%)
Chondrule	1.32	1.33	0.31	0.01	1.33	16.59
CAI	1.70	1.66	0.64	0.03	1.68	29.24
Rim	1.50	1.50	0.75	0.09	1.50	23.69
Matrix	-	-	-	-	1.40	20.09

Fry's Method. Is a point-to-point technique for determining whole rock deformation in anti-clustered samples such as sandstones and conglomerates [10]. This method was used to determine the whole rock strain and relative strike of the fabric. Spherical chondrules were selected over more irregular shaped CAIs, due to the greater predictability of their original aspect ratio [2,11]. Chondrules were run through ImageJ and an objective ellipse fitting plugin [12]. The results showed a long axis angle of 038° and an ellipse ratio of 1.4 (Fig. 1), this translates to a uniaxial shortening of 20% perpendicular to the long axis.
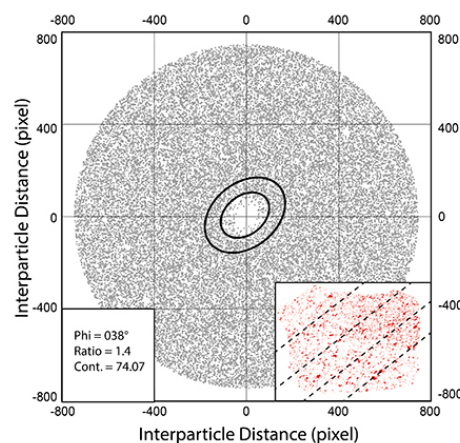
Fig. 1: Fry diagram for chondrules in the Tait dataset. The central ellipse records a strike of 038° and an axial ratio of 1.4. Inset: This represents the strike, overprinted on a slab of Allende with all the CAIs in red.

Flinn's Method. This technique measures the strain of a sample in 3D by plotting the strain axis of an ellipsoid X/Y and Y/Z [23]. This was done by digitizing encapsulated CAIs (n=19), from a stack of CT imagery of the Allende slab. An ellipsoid was fit to each of the CAIs using BoneJ [24]. The results showed axial ratios of X/Y = 1.42, Y/Z = 3.69, and X/Z = 5.26. This translates to a uniaxial shortening of 49% ± 12° (std. error). The shape descriptor *k* is used to describe

the shape of the strain ellipsoid, the value $k = 0.27$ puts it in the oblate field (Fig. 2). The average dip defined by the CAIs was: $17.56° \pm 1.96°$ (std. error) to the west, relative to the surface of the Allende slab.
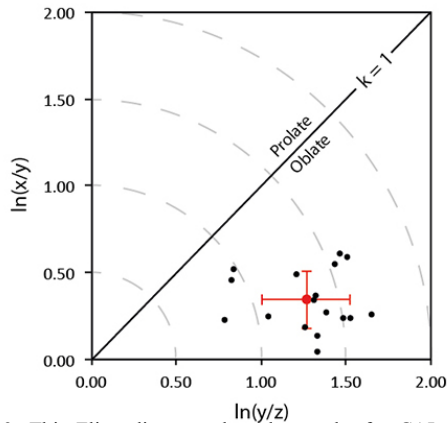
Fig. 2: This Flinn diagram plots the results for CAIs completely encapsulated in the CT data. All data points plot in the oblate (flattening field) with $k = 0.27$. The red value is the arithmetic mean.

SEM Element Map. Element maps were previously generated on a JEOL 7600F SEM with a pixel resolution of 3.23 μm/pixel [15]. The elements mapped were Ca (Green), Al (Blue) and Mg (Red). Images show an apparent long axis alignment of Ca-rich pyroxenes (~50 μm) surrounding particles. These pyroxene grains are contained in the matrix and are not part of the chondrule rims (Fig. 3a).
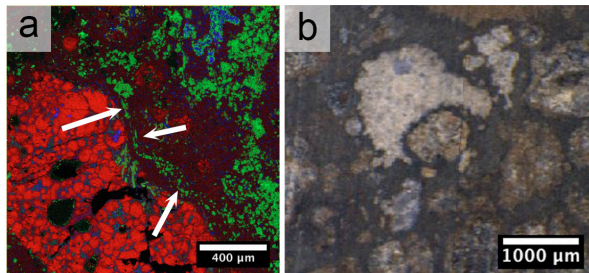
Fig. 3: (a) SEM element map data. Ca (Green), Al (Blue), Mg (red). 'augen' alignment of Ca-rich pyroxenes. Arrows point out deformation and long axis elongation. (b) Shows a photograph of a CAI wrapping around a more competent chondrule.

Discussion and Conclusions: *Strain Description.* Fry diagrams support a fabric with a strike of ~038° (relative to the image) and a dip to the "west" of ~17°. Not all phases have partitioned strain evenly (Table 1, Fig. 3b); CAIs record the most strain with a minimum uniaxial shortening of 29% and a maximum shortening of 49%. The maximum value is based on the assumption that CAIs were initially perfect spheres like the chondrules. Some preaccretionary deformation is likely given the ubiquity of irregularly shaped CAIs

surrounded by Wark-Lovering rims that formed prior to accretion. Nevertheless, the relative order of apparent strain partitioning is: CAIs > Rims > Matrix > Chondrules. Chondrules are the least strained of the phases $16.59\% \pm 0.58\%$ (std. error) which is probably due to their higher competency acting as porphyroblasts (Fig. 3b). Fry's method shows the matrix is deforming around the chondrules with an increased amount of shortening (20%), and "augen" alignments of secondary Ca-rich pyroxenes (Fig. 3a). These pyroxenes are believed to be secondary minerals [16] that grew in orientations defined by the deformed matrix. Deformation of the matrix has also been observed by other workers using EBSD [7,17]. The rims of chondrules show more strain partitioning than the chondrules themselves. If the rims were formed after deformation the ratio should be ~1.0 but given that the ratio is ~1.5, it would imply that the rim was emplaced prior to deformation (and likely accretion).

Strain Origin. The origin of the petrofabrics in Allende is still up for debate. Given that all phases exhibit shortening and the presence of augen in the matrix, an imbrication-only model is unlikely as such an alignment would have little bearing on the matrix [1]. Overburden is cited as an origin but little evidence in the literature supports this conclusion [4]. Hypervelocity impacts have been cited as possible formation mechanisms for the fabrics and have been showed experimentally to flatten chondrules [18]. Interestingly, these flattening experiments coincided with chondrule axial ratios of 1.34 for 11 GPa, very similar to the minimum value of 1.31 found here.

References: [1] R.T. Dodd Jr. (1965) *Icarus,* 4, 308. [2] D.S. Sneyd, et al. (1988) *Meteoritics,* 23, 139. [3] D. Stoffler, et al. (1991) *GCA,* 55, 3845. [4] P.M. Cain, et al. (1986) *EPSL,* 77, 165. [5] D.S. Sneyd, et al. (1985) *LPSC XVI,* 797–798. [6] L.E. Watt, et al. (2006) *MetSoc,* 41, 989. [7] P.A. Bland, et al. (2003) *Met. Soc. LXVI.* [8] P. Srinivasan, et al. (2013) LPSC XLIV. [9] W.S. Rasband. (1997) *U.S. Nat. Ins. Health.* [10] N. Fry. (1979) *Tectonophysics,* 60, 89. [11] P.M. Martin, A.A. Mills. (1976) *EPSL* 33, 239. [12] J.W. Waldron, K.D. Wallace. (2007) *J. Struc. Geol.,* 29, 1430. [13] D. Flinn. (1962) *Q. J. Geol. Soc.,* 118, 385. [14] M. Doube, et al. (2010) *Bone,* 47, 1076. [15] P. Christofferson, et al. (2012) LPS XLIII. [16] A.N. Krot, et al. (1998) *MetSoc,* 33, 623. [17] P.A. Bland, et al. (2011) *Nature Geosci.,* 4, 244. [18] T. Nakamura, et al. (1995) *Meteoritics,* 30, 34.